◆ Human Brain Mapping 7:67–77(1999) ◆

Perception of First- and Second-Order Motion: Separable Neurological Mechanisms?

Lucia M. Vaina,[1,3*] Alan Cowey,[2] and David Kennedy[1,3]

[1]*Brain and Vision Research Laboratory, Department of Biomedical Engineering and Neurology, Boston University and Harvard Medical School, Department of Neurology, Brigham and Women's Hospital, Boston, Massachusetts, USA*
[2]*University of Oxford, Department of Experimental Psychology, Oxford, UK*
[3]*Center for Morphometric Analysis, Massachusetts General Hospital, Charlestown, Massachusetts, USA*

Abstract: An unresolved issue in visual motion perception is how distinct are the processes underlying "first-order" and "second-order" motion. The former is defined by spatiotemporal variations of luminance and the latter by spatiotemporal variations in other image attributes, such as contrast or depth. Here we describe two neurological patients with focal unilateral lesions whose contrasting perceptual deficits on psychophysical tasks of "first-order" and "second-order" motion are related to the maps of the human brain established by functional neuroimaging and gross anatomical features. We used a relatively fine-grained neocortical parcellation method applied to high-resolution MRI scans of the patients' brains to illustrate a subtle, yet highly specific dissociation in the visual motion system in humans. Our results suggest that the two motion systems are mediated by regionally separate mechanisms from an early stage of cortical processing. *Hum. Brain Mapping. 7:67–77, 1999.* © 1999 Wiley-Liss, Inc.

Key words: Visual motion deficits; neurological patients; first and second order motion; cortical parcellation

INTRODUCTION

The occipital and preoccipital cortex in primates comprises a large number of extrastriate visual areas that can be delineated topographically and functionally. Several of these areas are specialized for the analysis of visual motion, and physiological, behavioral, and anatomical studies of these extrastriate areas in macaque monkeys concur in demonstrating that the motion-responsive areas are organized in a system of interacting functional pathways that originate in the primary visual cortex and have their principal distribution in the cortex of the posterior parietal lobe [for review, see Boussaoud et al., 1990; Wurtz et al., 1990; Felleman and van Essen, 1991; Ungerleider, 1996]. Recently, functional neuroimaging by PET and fMRI in human subjects has provided additional evidence that, as suggested by single-cell studies in macaque monkeys, discrete areas in the human extrastriate cortex are

Contract grant sponsor: NIH; Contract grant number: 2EY07861–3 (L.M.V.); Contract grant sponsor: Oxford McDonnell-Pew Network (A.C. and L.M.V.); Contract grant sponsor: MRC; Contract grant number: G971/397/B (A.C.).

*Correspondence to: Professor Lucia M. Vaina, Boston University, Brain and Vision Research Laboratory, Department of Biomedical Engineering, 44 Cummington Street, Boston, MA 02215, USA. E-mail: vaina@enga.bu.edu

Received 29 January 1998; accepted 23 June 1998

selectively engaged in the analysis of different aspects of visual motion. With due caution, bearing in mind known differences between the cortical organization of the two species [for a review, see Tootell et al., 1996], the functional neuroimaging studies have provided several candidates as human homologs of the motion areas described in the macaque [e.g., Dupont et al., 1994; Orban et al., 1995; Tootell et al., 1995, 1996; Watson et al., 1993; Ungerleider, 1996; Zeki et al., 1991].

Cortical maps are helpful in describing the components and likely interactions within the system dealing with visual motion, but alone they do not yet provide unambiguous information about the contrasting *behavioral* role of different visual areas in the perception of different types of visual motion. While many motion areas have been mapped, we remain uncertain of their precise behavioral function. In the absence of any other noninvasive means of establishing functional roles for different areas of the human extrastriate cortex, the study of patients with selective perceptual deficits caused by focal lesions that can be related to established cortical maps offers a special opportunity to correlate structure and function. In this article, we describe two patients whose contrasting perceptual deficits on two types of visual motion is related to the maps of the human brain established by functional neuroimaging and gross anatomical features. We use psychophysics and structural neuroimaging to illustrate a subtle dissociation in the visual motion system in humans.

The performance of two patients, FD and RA, on an extensive set of psychophysical tests designed to evaluate motion perception has revealed a clear double dissociation of deficits. Patient RA [described in detail in Vaina et al., 1998] showed severe impairment on those tests where detection of direction of motion is luminance-based; that is, it depends on spatiotemporal correlation of intensity in the visual field. This motion mechanism is referred to as first-order, or Fourier motion, in contrast to the second-order mechanism, which mediates the perception of motion that has no overall directional component in the Fourier domain, i.e., where there is no consistent difference in luminance between the moving elements and their background in the image. The first-order motion mechanisms are therefore blind to the second-order motion because the latter contains no consistent difference in luminance, although there is a difference in other stimulus attributes, such as contrast [Chubb and Sperling, 1988]. Yet psychophysics has convincingly demonstrated that normal human observers have no trouble in perceiving purely second-order motion. Interestingly, patient RA's performance was normal on tests of second-order motion, in spite of his severe and lasting deficits on a large number of tests of first-order motion. On the other hand, patient FD, described in detail by Vaina and Cowey [1996], performed normally on first-order motion tests, but showed severe impairment on second-order motion tasks in which the direction of motion resulted from a difference in image attributes other than luminance. The main purpose of the present article is, therefore, to compare the anatomical locus of the lesions that impair the two types of motion where the patients were given identical psychophysical tests. A preliminary report has been published as an abstract [Vaina et al., 1996].

The nature of these two motion systems and their interaction have been addressed in many psychophysical studies [Ledgeway and Smith, 1994; Lu and Sperling, 1995; Werkhoven et al., 1993; for review, see Clifford and Vaina, 1998]. Several of these studies suggest that in order to perceive second-order motion, a squaring nonlinearity must precede the extraction of motion information from second-order motion stimuli, whereas the first-order process computes the motion signal directly by spatiotemporal Fourier filtering of signals proportional to the local retinal illuminance [Chubb and Sperling, 1988; Wilson et al., 1992; Boulton and Baker, 1993]. There is also physiological evidence [Albright, 1992; O'Keefe and Movshon, 1996; O'Keefe et al., 1993] for the existence of neurons in the middle temporal (MT) and superior polysensory (STP) areas in macaque monkeys that are sensitive to second-order motion. Zhou and Baker [1993], recording from areas 17 and 18 in cats, demonstrated a pathway selectively responsive to second-order motion. In the normal human brain, functional activations evoked by first- or second-order motion displays are spatially coincident [Somers et al., 1998], although those induced by second-order motion were stronger in area V3 [Smith et al., 1998]. Yet the psychophysical and neuropathological data from the patients reviewed here, RA and FD, support the hypothesis of two regionally separable dissociable mechanisms mediating first- and second-order motion. Patient RA has a focal lesion in the medial part of the occipital lobe, whereas FD has a lesion in the dorso lateral part of the junction between occipital and temporal lobe. In view of the apparent inconsistencies, we analyzed FD's lesion in greater detail and with the same method used to describe RA's. We first describe the lesion localization, using a neocortical parcellation method, and then summarize

RA's and FD's neurological and neuropsychological background and performance on tests of motion perception.

METHODS

Tests were carried out on two neurological patients and a larger group of healthy volunteers. All subjects, including the patients, gave informed consent to participate in the study, which had the approval of Boston University Human Subjects Committee.

Patient FD, a male, right-handed college-educated social worker, suffered a left hemisphere infarct of uncertain etiology in 1992, at the age of 41. Neurological examination revealed slight right-sided weakness, lasting a few days, and a mild anomia lasting a few weeks. He complained of feeling disturbed by visually cluttered moving scenes or noisy surroundings. Neuro-ophthalmological examination, including visual fields, was normal and his uncorrected visual acuity was 20/20 in both eyes. Contrast sensitivity for detection of static or moving gratings and for discrimination of direction and speed of motion were normal, as was temporal frequency discrimination. Discrimination of spatial relations, stereopsis, color orientation, 2-D form from luminance, direction or speed of motion, and perception of 3-D structure from motion were all normal for a wide range of stimulus conditions. His scores on the performance scale of the Wechsler Adult Intelligence Scale, Revised (WAIS-R) (PIQ = 97) was average for his age and education level.

Patient RA is a right-handed retired computer manager who suffered a sudden right hemisphere embolic stroke in January, 1994, at the age of 66. For three weeks his speech was slurred and his left arm and, to a lesser extent, his left leg were weak. On neurological examination he also had depressed sensation in his left arm and leg. On the neuropsychological evaluation with the performance scale of the WAIS-R, his score was in the average range for his age and education (PIQ = 92). His vocabulary and basic language skills were normal. Visual fields obtained by both Goldmann and Humphrey perimetry revealed a left inferior quadrantopia. This resolved over a period of 16 months, when the behavioral data presented here were obtained.

MRI acquisition

Magnetic resonance imaging (MRI) studies of the patients' brains were obtained using a 1.5 Tesla GE Signa System (GE Medical Systems, Milwaukee, WI) without intravenous contrast enhancement. Sagittal T1-weighted axial proton density and T2-weighted images (3 mm thick, no gap) were obtained first, followed by an additional set of coronal SPGR (spoiled gradient echo sequence) 124 contiguous 1.5-mm thick images. Imaging parameters were FOV 24 cm, interleaved acquisition, TR 3000 ms, and Te 80 ms, acquisition matrix = 356 × 256. The first echo was acquired with a Te of 30 ms proton sensitivity weighted images. Data acquired in 3-D raster metrics (SD Fourier transfer spoiled gradient-recalled acquisition in steady state) were stored in coronal images.

Anatomical analysis of brain images

Positional normalization

A coordinate system is defined for the MR image dataset for each brain such that the Y axis corresponds to the anterior commissure – posterior commissure line. The Z (superior–inferior) axis is set orthogonal to the Y axis, passing through the interhemispheric fissure, and the X (medial–lateral) axis is orthogonal to both Y and Z axes [Filipek et al., 1994; Talairach and Tournoux, 1988]. The X–Z axes specify the coronal plane, while the Y–Z axes specify the sagittal plane and the Y–X axes specify the transaxial image plane within this coordinate system. A new set of coronal planes are reconstructed according to the above coordinate system with plane thickness of 1.5 mm. Cerebral cortex outlines, including fissures, are created for all coronal levels posterior to the posterior commissure [Filipek et al., 1994]. This neocortical ribbon serves as the basis for the cortical parcellation.

Neocortical parcellation

The segmented neocortical ribbon of each hemisphere is subdivided by topographic criteria into parcellation units (PU) according to a three-step procedure [Caviness et al., 1996; Rademacher et al., 1992]. First, the anterior and posterior borders of parcellation units are defined by coronal planes determined by the positions of a set of 42 anatomic landmarks (principally points of intersection of fissures). Second, the lateral and medial borders of parcellation units are defined by the 31 trajectories of fissures. Third, the appropriate name is assigned to each parcellation unit [Caviness et al., 1996]. While these regions are not necessarily analogs of individual functional or cytoar-

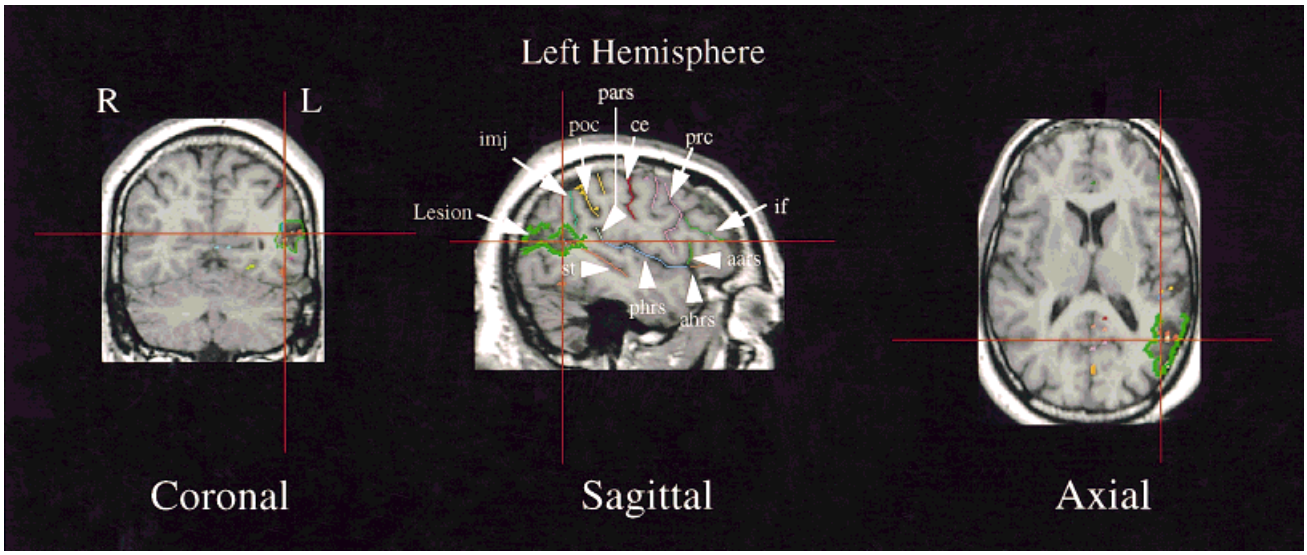

Figure 1.
Example of the anatomic cross-referencing and localization analysis, demonstrated in patient FD. Normalized coronal, sagittal and axial reconstructions are shown; cross-reference lines in each image indicate the levels shown in the other two views. The lesion is identified in each of these views, and the sagittal view demonstrates the complete sulcal identification.

chitectonic areas, they do correlate with a specific subset of them. The parcellation system is relatively fine-grained. It retains the principal topographic landmarks that have traditionally stood as reliable mapping guides in cognitive neuroscience. The nomenclature for the system is exclusively topographic, arising entirely from the landmarks that can be seen, and a traditional vocabulary is applied to these landmarks. A notable advantage of this method is that the regions are unambiguously definable in a standardized fashion from high-resolution MRI. The method uses an interactive software package which facilitates multiplanar displays for cortical landmark identification in the three orthogonal cardinal views (axial, sagittal, coronal) of a volumetric dataset. The criteria for locating the landmarks upon which the parcellation is based are robust and previous experience establishes that practiced investigators can parcellate the cerebrum reliably and efficiently using the computer image analysis routines [Caviness et al., 1996].

Lesion identification

The spatial extent of the lesion was outlined on each slice where it was identified. In both patients RA and FD, the lesion was small enough not to disrupt the identification of the requisite sulcal trajectories and landmarks. Therefore, the localization of the lesion can be accomplished in the cortical parcellation system by the identification of the overlap between the lesion outlines and the cortical parcellation unit outlines. The relative topography of each lesion can be illustrated on the idealized parcellation template [Caviness et al., 1996; Rademacher et al., 1992].

Methods of psychophysical assessment

The psychophysical methods are described in detail in Vaina and Cowey [1996]. Briefly, all visual stimuli were displayed on a Macintosh 13 inch color monitor (active viewing area 235 × 176 mm), and responses collected and analyzed using a Macintosh Quadra 650 computer. The experiments took place in a quiet dark room, in which the only appreciable illumination came from the testing display. Subjects sat 60 cm from the screen and fixated a small black fixation mark at eye-level, 2° to the left or right of the imaginary margin of the display, which the subject viewed binocularly. Subject's responses were verbal and the examiner entered them on the computer. Test difficulty was

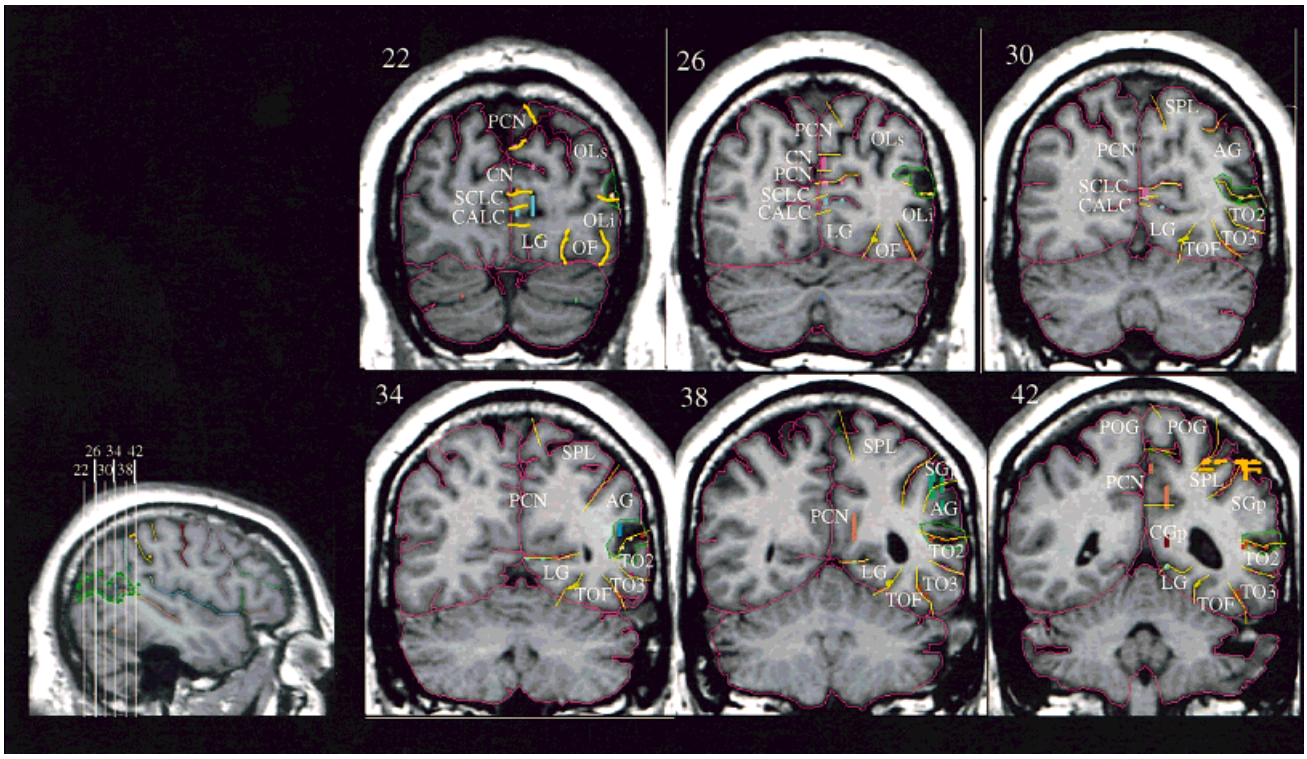

Figure 2.
Coronal MR images showing the lesion in patient FD on the lateral surface of the left occipital lobe (shown on right). Damage to white matter is slight, but the lesion involves both banks of the superior temporal sulcus from slices 30–42 and the lateral ventricle is enlarged on that side. The anterior–posterior position of the coronal slices is shown at bottom left

titrated using an adaptive staircase procedure [Saiviroporoon, 1992; Vaina et al., 1998] and threshold for each run was computed as the arithmetic mean of the last six reversals, and the threshold for each type of test was taken as the mean of the thresholds from two runs. In the figures, the results are plotted as filled circles for the right visual hemifield and unfilled circles for the left hemifield.

RESULTS

Lesion localization

Figure 1 demonstrates the cortical parcellation method as applied to patient FD. In patients with small cortical and subcortical lesions, the anatomic cross-referencing method permits accurate identification of major sulci and lesion extent. These observable features provide the basis of the cortical parcellation localization system. Figures 2 and 3 show the results of the application of this system to patients FD and RA, respectively. In each of these sets of coronal images, the cerebral hemispheres and lesion are outlined, the major fissures are traced, and the parcellation units are identified. In patient FD (Fig. 2) the lesion is located dorso-laterally in the left hemisphere and is almost entirely cortical. The lesion starts posteriorly on the superior temporal sulcus and involves both the superior (OLs) and inferior (OLi) occipital lateral cortex. It extends anteriorly to include portions of the angular gyrus (AG) and middle temporal-occipital cortex (TO2), and terminates in the inferior portion of the posterior supramarginal gyrus (SGp). In patient RA (Fig. 3), the lesion is located medially in the right hemisphere and involves cortical and white matter of the medial parcellation units. From posterior to anterior, it begins in the occipital pole, extends to involve the cuneus (CN) and supracalcarine cortex (SCLC), and then

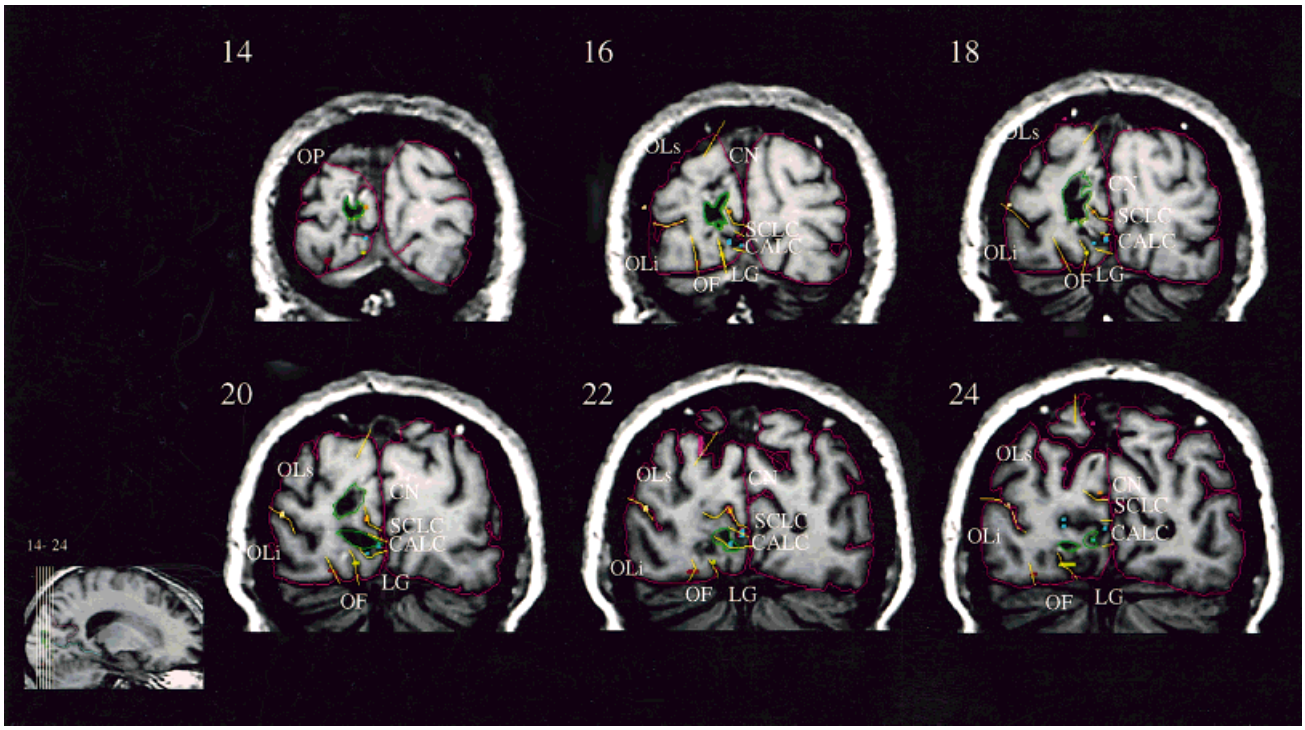

Figure 3.

Coronal MR images showing the lesion in patient RA in relation to the cortical parcellation units. The outline of the occipital cortex is shown in red and the outline of the lesion in green. From slices 14–18 the lesion is predominantly dorsal to the striate cortex of the calcarine sulcus, whereas in slices 22–24 it extends ventrally, below the calcarine sulcus to the lingual gyrus. The anterior–posterior position of the coronal slices is shown at bottom left.

descends to include portions of the calcarine cortex (CALC) and the lingual gyrus (LG).

Psychophysical results: Motion perception in RA and FD

Figure 4 on the left (a,c,e) shows schematic views of three first-order motion discrimination tasks: speed, direction, and motion coherence. On the right (b,d,f) are shown the performance on each of these tasks of normal controls, and RA and FD. RA was impaired on all three tests for stimuli presented in the left visual field, contralateral to the lesion. FD's performance was normal on all the tests in both hemifields. Although the first two tasks are spatially local, the Motion Coherence test, shown schematically in Figure 4e, is a spatially global task, since to determine the direction of motion, subjects must spatially integrate motion signals throughout the stimulus field. This type of display was used by Newsome and Pare [1988], who showed that neurotoxic lesions of visual area MT in monkeys increased the proportion of coherence necessary for discriminating direction of motion. RA was mildly impaired in both hemifields with this stimulus and remained so on the several occasions he was tested over the next two years, always hovering around 20% coherence. FD's performance changed over time. Initially he was impaired in the visual field contralateral to the lesion, but had recovered within two months. Notably, this global task was the *only* first-order motion task on which FD was impaired from the extensive array of tests used to evaluate his motion perception in the first few weeks.

The performance of the two patients on second-order motion was oppositely dissociated. Figure 5 shows schematically a task of second-order motion [adapted from Albright, 1992] in which discrimination of direction is based on flicker-defined contrast. A varying percentage of randomly flickering dots within an imaginary square-wave grating drifts upwards or downwards, superimposed on a static dense random dot pattern. The flickering was created by randomly

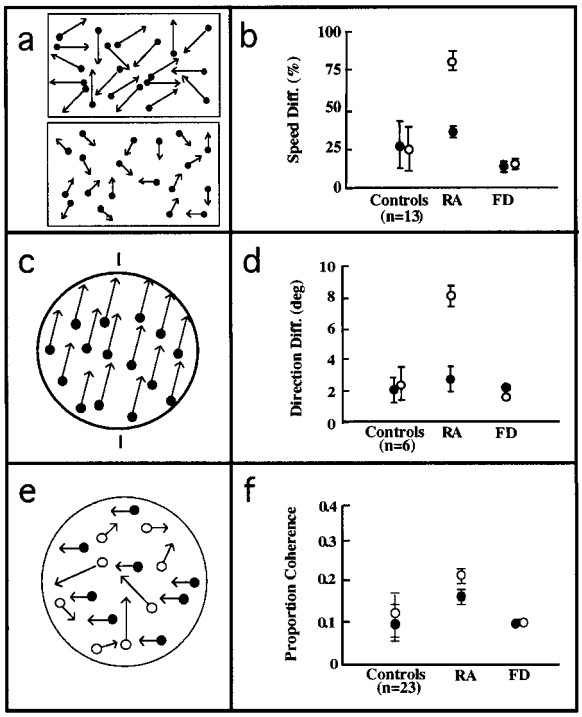

Figure 4.

(**a, b**) The scheme and results of a speed discrimination task. The display contains two clouds of dots presented in two apertures arranged one under the other. Within each aperture the dots move in random directions, but in one of the apertures, top or bottom, they move faster. In a 2AFC task and using a staircase procedure, subjects had to report in which aperture the dots move faster. Although we present only one set of data from RA, his performance remained consistent over 2 years. Moreover, this performance did not change even after his initial quadrantic visual field deficit had recovered. The direction discrimination task (**c, d**) presented a field of evenly distributed dots all moving in the same direction, either slightly to the right or to the left of an imaginary vertical line (two small lines placed outside the stimulus indicated true vertical). Using a staircase procedure, the subject was shown these stimuli in 2AFC paradigm. Subjects fixated 2° off the lateral edge of the stimulus at midline level. The y axis indicates the smallest angular difference from vertical needed for reliable discrimination of direction of motion. (**e, f**) Test of perception of motion coherence. Schematic view of the displays used for first-order global motion. On the left (**e**) is a typical trial where a proportion of the dots (the filled circles) move in one direction while the others provide masking noise. The algorithm for generating this stimulus [adapted from Newsome and Pare, 1988] freshly assigns the direction of each dot in each frame; that is, during one trial only the proportion of dots that move in a specific direction is the same, but not the dot identity. (**f**) Patient FD was unimpaired on this task 2 months after his lesion, whereas patient RA was impaired in the hemifield contralateral to his lesion.

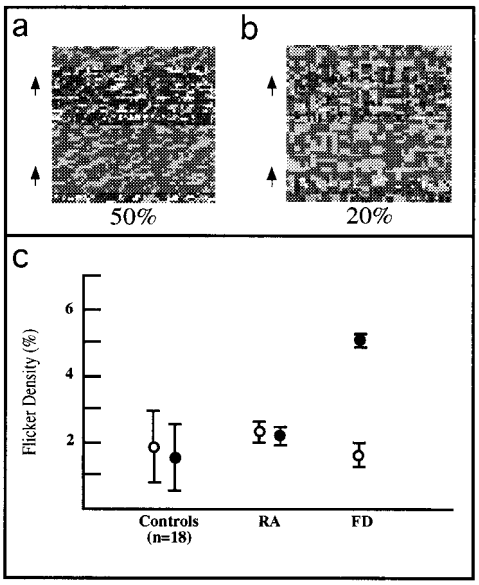

Figure 5.

(**a, b**) Two individual forms of the display used to create second-order motion from flicker. The dots are static but the position of the bar in which some proportion of them flicker shifts up or down. The percentage of flickering dots was varied and is 50% in (**a**) and 20% in (**b**). As shown in (**c**), patient FD required a much higher percentage of flickering dots in his impaired hemifield in order to discriminate direction of motion, whereas RA did not.

inverting the contrast of a given percentage of dots in each 15 ms frame within alternate stripes of the grating. Thus, there was no first-order luminance cue in the stimulus. The percept is a twinkling horizontal bar drifting smoothly up or down. In a two-alternative forced-choice paradigm, the subject had to indicate the direction of motion, upward or downward. Figure 5c shows that RA was normal, while FD was impaired on the task when the stimulus was presented in the visual field contralateral to his lesion.

Figure 6 illustrates a first-order and second-order global motion task that is conceptually similar to the motion coherence test of Figure 4e. The background consisted of flickering random dots and subjects had to perform a direction discrimination (left or right) in stochastic first-order (Fig. 6a) or second-order (Fig. 6c) displays in which a variable proportion of the "tokens" (i.e., small binary black and white texture patches) move coherently, left or right, while the others are presented from frame to frame at random location within the aperture. In the first-order version of the

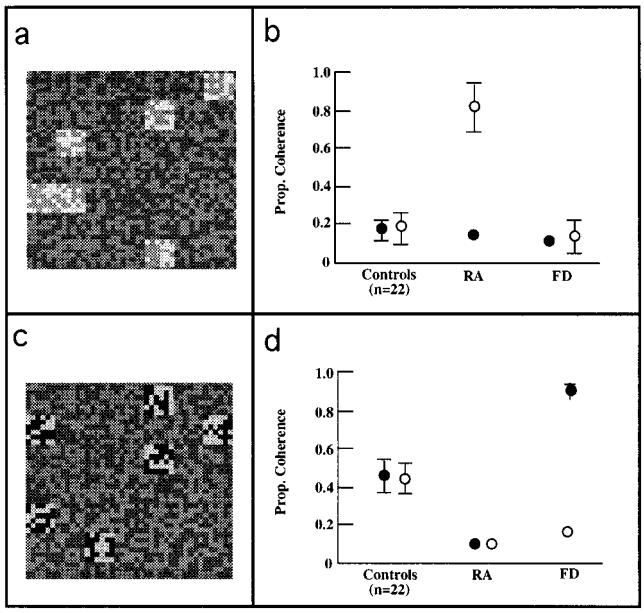

Figure 6.

Examples of first-order (**a**) and second-order (**c**) global motion using flickering random dots. In (**a**) the tokens (small clusters of pixels) differ in mean luminance from the surround. In (**c**) the tokens differ from the surround in contrast but not in mean luminance. RA was impaired in his affected hemifield on the first-order task (**b**), whereas FD was impaired in his affected hemifield on the second-order task (d)

stimulus (a), there is a difference between the mean luminance of the tokens and the background while the contrast is identical. In the second-order version, the tokens differ in mean contrast from the background but not in mean luminance. Figure 6b and d shows that in the visual hemifield contralateral to the lesion, RA was impaired with first-order motion but not second-order, whereas FD showed the opposite dissociation.

DISCUSSION

The performance of RA and FD on the psychophysical tasks described above demonstrate a double dissociation of deficits of first- and second-order motion.

An impairment on second-order motion discrimination has been described by Plant et al. [1993] and Greenlee and Smith [1997]. The latter study found that direction thresholds were slightly more elevated for second-order stimuli than for first-order stimuli, whereas the reverse was true for speed discrimination. However, they concluded that there is extensive overlap in the cortical areas involved in the two kinds of motion processing. While not disagreeing with the latter, the results presented here show that functional segregation can be demonstrated when the lesions are much farther apart.

Figure 7 shows a schematic representation of RA and FD's lesions in the cortical parcellation system. RA's lesion is situated within the medial half of the occipital lobe, especially above the calcarine sulcus caudally but also below it more rostrally. In addition, it involves and to some extent ''undercuts'' the cuneal sulcus. FD's dorsolateral lesion involves the cortex of the superior and inferior banks of the caudal portion of the superior temporal sulcus in the left hemisphere. It is more extensive than RA's lesion rostro-caudally but much more superficial, involving almost exclusively gray matter.

The functional neuroimaging studies of Watson et al. [1993] and Tootell et al. [1995] place the human analog of the macaque area MT more ventrally than FD's lesion but closely adjacent to it. It thus appears that area MT was spared by the lesion, suggesting that an intact area MT is not itself sufficient for perception of second-order motion despite unaltered perception of first-order motion. The lesion in RA is more difficult to allocate to any extra-striate visual area or areas but the cortex directly involved almost certainly includes area V3, both above and below V1 in the calcarine sulcus, and V2 on the medial surface [Clarke and Miklossy, 1990]. As well, it slightly involves white matter and could, therefore, have disrupted connections between V1 and regions of the dorsal set of visual areas whose neurons, in monkeys, are selective for a variety of motion stimuli. For example, both areas MT and PO in macaque monkeys, although widely separated, receive a prominent direct projection from V1. The fact that RA was conspicuously unimpaired with our tasks of second-order motion (including several not described here) reinforces the proposal that the two motion systems are mediated by regionally separate mechanisms from an early stage of cortical processing.

This appears to be inconsistent with the results of a recent fMRI study by Smith et al. [1998], who report that the areas V3 and VP show stronger responses to second-order than to first-order motion, suggesting that these might be the first cortical areas that explicitly represent second-order motion. Even if this hypothesis were correct, it is conceivable that since area VP was clearly not involved in RA's lesion, he might have used it in processing the second-order motion stimuli. Area VP is connected to other motion areas that are rich in direction-selective neurons; for example, area MT [Fel-

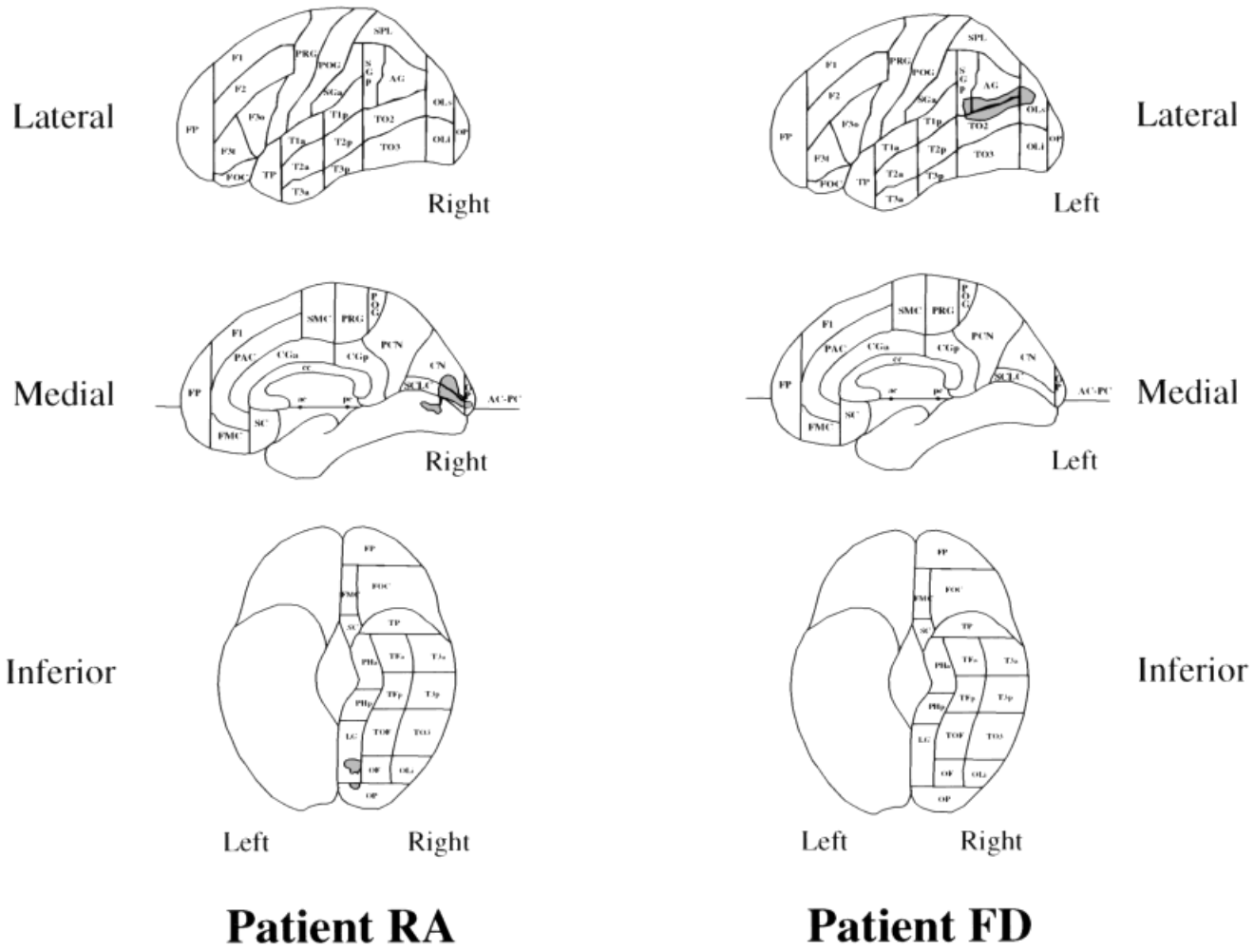

Figure 7.
Comparison of the lesion localization using the cortical parcellation system of Rademacher et al. [1992] in the two patients. The lesion in patient RA involves cortical parcellation units CALC, SCLC, CN, LG, and OP in the right hemisphere. In patient FD it involves cortical parcellation units SGp, AG, and TO2 in the left hemisphere.

leman and van Essen, 1991], which is known to respond to direction of motion no matter what the nature of the cues by which motion is defined [e.g., first-order or second-order, Albright, 1992; O'Keefe and Movshon, 1996]. This could explain RA's normal performance on a broad range of direction discrimination tasks of second-order motion. Moreover, the involvement in his lesion of areas V2 and V3, both known to contribute to the analysis of first-order stimuli and to project to MT and other higher motion areas, may explain his severe impaired performance on the first-order counterpart of the second-order direction discrimination tasks.

The next productive step in analyzing the functional neuroanatomy of the two systems would be to localize the lesions in FD and RA to functional rather than to anatomical landmarks; for example, by retinotopic mapping of areas V1, V2, V3, V4, and V5, as now so clearly demonstrated in undamaged brains [De Yoe et al., 1996; Engel et al., 1997; Sereno et al., 1995; Tootell et al., 1998]. It will be equally important to use a much larger range of first- and second-order displays, including the types described here, in further studies of cortical activation, given that both types can be created in several ways (e.g., local and global) and might engage different cortical visual areas.

ACKNOWLEDGMENT

We thank Jose Diaz for programming the psychophysical stimuli.

REFERENCES

Albright TD (1992): Form-cue invariant motion processing in primate visual cortex. Science 255:1141–1143.

Boulton JC, Baker CL (1993): Different parameters control motion perception above and below a critical density. Vision Res 33:1803–1811.

Boussaoud D, Ungerleider LG, Desimone R (1990): Pathways for motion analysis: Cortical connections of the medial superior temporal and fundus of the superior temporal visual areas in the macaque. J Comp Neurol 296:462–495.

Caviness VS Jr, Makris N, Meyer J, Kennedy DN (1996): MRI-based parcellation of human neocortex: An anatomically specified method with estimate of reliability. Cereb Cortex 6:726–736.

Chubb C, Sperling G (1988): Drift-balanced random stimuli: A general basis for studying non-Fourier motion perception. J Opt Soc Am A 5:1986–2007.

Clarke S, Miklossy J (1990): Occipital cortex in man: Organization of callosal connections, related myelo-and cytoarchitecture, and putative boundaries of functional visual areas. J Comp Neurol 298:188–214

Clifford WGC, Vaina LM (1998): A computational model of selective deficits in first- and second-order motion processing. Vision Res (in press).

De Yoe EA, Carman G, Bandettini PA, Glickman S, Cox R, Miller D, Neitz J (1996): Mapping striate and extrastriate visual areas in human cerebral cortex. Proc Natl Acad Sci USA 93:2382–2386.

Dupont P, Orban GA, De Bruyn B, Verbruggen A, Mortelmans L (1994): Many areas in the human hrain respond to visual motion. J Neurophysiol 72(3):1420–1424.

Engel SA, Glover GH, Wandell BA (1997): Retinotopic organization in human visual cortex and the spatial precision of functional MRI. Cereb Cortex 7:181–192.

Felleman DJ, Van Essen DC (1991): Distributed hierarchical processing in the primate cerebral cortex. Cereb Cortex 1(1):1–47.

Filipek PA, Richelme C, Kennedy DN, Verne J, Caviness S (1994): The young adult human brain: An MRI-based morphometric analysis. Cereb Cortex 4(4):344–260.

Greenlee MW, Smith AT (1997): Detection and discrimination of first- and second-order motion in patients with unilateral brain damage. J Neurosci 17:804–818.

Ledgeway T, Smith AT (1994): Evidence for separate motion-detecting mechanisms for first- and second-order motion in human vision. Vision Res 34:2727–2740.

Lu ZL, Sperling G (1995): The functional architecture of human visual motion perception. Vision Res 35:2697–2722.

Newsome WT, Pare EB (1988): A selective impairment of motion perception following lesions of the middle temporal visual area (MT). J Neurosci 8:2201–2211.

O'Keefe LP, Movshon JA (1996): Processing of first- and second-order motion signals by neurons in area MT of the macaque monkey. Vis Neurosci 15:305–317.

O'Keefe LP, Carandini M, Beusmans JMH, Movshon JA (1993): MT neuronal responses to 1st- and 2nd-order motion. Soc Neurosci Abstr 19:1283.

Orban GA, Dupont P, De Bruyn B, Vogels R, Vandenberghe R, Mortelmans L (1995): A motion area in human visual cortex. Proc Natl Acad Sci USA 92:993–997.

Plant GT, Laxer KD, Barbaro NM, Schiffman JS, Nakayama K (1993): Impaired visual motion perception in the contralateral hemifield following unilateral posterior cerebral lesions. Brain 116:1337–1353.

Rademacher J, Galaburda AM, Kennedy DN, Filipek PA, Caviness VS (1992): Human cerebral cortex: Localization, parcellation, and morphometry with magnetic resonance imaging. J Cogn Neurosci 4(4):352–374.

Saiviroporoon P (1992): A computerized instrument for the diagnosis of visual deficits in humans. M.S. Thesis, Department of Biomedical Engineering, Boston University.

Sereno MI, Dale AM, Reppas JB, Kwong KK, Belliveau JW, Brady TJ, Rosen BR, Tootell RBH (1995): Borders of multiple visual areas in humans revealed by functional magnetic resonance imaging. Science 268:889–893.

Smith AT, Greenlee MW, Singh KD, Kraemer FM, Hennig J (1998): The processing of first- and second-order motion in human visual cortex assessed by functional magnetic resonance imaging (fMRI). J Neurosci 18:3816–3830.

Somers DC, Seiffert AE, Dale AM, Tootell RBH (1998): fMRI analysis of second-order visual motion perception and attentive tracking. NeuroImage 7:S323.

Talairach J, Tournoux P (1988): Co-Planar Sterotaxic Atlas of the Human Brain. New York: Georg Thieme Verlag.

Tootell RBH, Reppas JB, Kwong KK, Mallach R, Born RT, Brady TJ, Rosen BR, Belliveau JW (1995): Functional analysis of human MT and related visual cortical areas using magnetic resonance imaging. J Neurosci 15(4):3215–3230.

Tootell RBH, Dale AM, Sereno MI, Malach, R (1996): New images from human visual cortex. Trends Neurosci 19(11):481–489.

Tootell RBH, Hadjikhani NK, Mendola JD, Marrett S, Dale AM (1998): From retinotopy to recognition: fMRI in human visual cortex. Trends Cogn Sci 2:174–183.

Ungerleider LG (1996): What and where in the human brain? Evidence from human functional brain imaging studies. In: Carminiti R, Hoffmann K-P, Lacquanti F, Altman J (eds): Vision and Movement Mechanisms in the Cerebral Cortex. Strasbourg: Human Frontiers Science Programme Organization, pp 23–30.

Vaina LM, Cowey A (1996): Impairment of the perception of second order motion but not first order motion in a patient with unilateral focal brain damage. Proc Roy Soc Lond B 263:1225–1232.

Vaina LM, LeMay M (1993): Deficits of non-Fourier motion perception in a patient with normal performance on short-range motion tasks. Soc Neurosci Abstr 19:1284.

Vaina LM, Makris N, Kennedy D, Cowey A (1996): The neuroanatomical damage producing selective deficits to first or second order motion in stroke patients provides further evidence for separate mechanisms. NeuroImage 3:S360.

Vaina LM, Makris N, Kennedy D, Cowey A (1998): The selective impairment of the perception of first-order motion by unilateral cortical brain damage. Vis Neurosci 15:333–348.

Watson JDG, Meyers R, Frackowiak RS, Hajnal JV, Woods RP, Mazziotta JC (1993): Area V5 of the human brain: Evidence from a combined study using positron emission tomography and magnetic resonance imaging. Cereb Cortex 3:79–94.

Werkhoven P, Sperling G, Chubb C (1993): The dimensionality of texture-defined motion: A single channel theory. Vision Res 33:463–486.

Wilson HR, Ferrera VP, Yo C (1992): A psychophysically motivated model for two-dimensional motion perception. Vis Neurosci 9:79–97.

Wurtz RH, Yamasaki DS, Duffy CJ, Roy JP (1990): Functional specialization for visual motion processing in primate cerebral cortex. Cold Spring Harbor Symposium on Quantitative Biology, Volume LV, pp 717–727.

Zeki S, Watson JDG, Lueck CK, Friston KJ, Kennard C, Frackowiak RSJ (1993): A direct demonstration of functional specialisation in human visual cortex. J Neurosci 11:641–649

Zhou Y-X, Baker CLB Jr (1993): A processing stream in mammalian visual cortex neurons for non-Fourier responses. Science 261:98–101.